# STUDY OF THE PORE STRUCTURE, PERMEABILITY, AND STRENGTH OF MATERIALS OF GRADES UPA-3 AND UPA-4

**G. M. Butyrin,**[1] **A. K. Protsenko,**[1] **and G. E. Mostovoi**[1]

Results are presented from a study of the changes in characteristics of the pore structure, gas permeability, and mechanical properties of materials UPA-3 and UPA-4, which are based on knitted and fabric fillers. The textiles of the materials have different structures and are based on carbon fibers (which are obtained using oxidized polyacrylonitrile and different grades of viscose). The changes in the characteristics are examined in relation to the degree of pre-compression of the materials and the length of time that they undergo compaction with pyrolytic carbon and graphite.

## INTRODUCTION

Reinforced pyrolytic carbon of grades UPA-3 and UPA-4 are carbon-carbon composites (CCCs) based on a carbonaceous fibrous reinforcing filler and a combination matrix whose main components are pyrolytic carbon (PC) and pyrolytic graphite (PG). The composites are characterized by high strength at high temperatures and resistance to thermal stresses in the presence of large temperature gradients. These properties are attributable to the highly oriented crystalline structure of the PG, this structure being created when the graphite is formed by the deposition of carbon onto the framework of the product. The framework is composed of carbon fibers which are in the form of knitting, knit cloth, or fabric that has previously been bound with PC. The PG framework is subsequently subjected to compaction, which makes the outer surface of the refractory product nearly pore-free [1, 2].

Products made of these materials — crucibles 500 mm in diameter and 900 mm high, pots, cathodes 200 mm in diameter and 900 mm high, tubes with a diameter of 210 mm, length of 950 mm, and wall-thickness of 12 mm, and plates with the dimensions $800 \times 400 \times 17$ mm — are used to melt various metals and alloys that may be aggressive and/or ultrapure. The refractory products are also used to recrystallize oxides of elements of the actinium group, this

being done either in an inert medium at temperatures up to 2000°C or in air at temperatures up to 550°C.

The materials' low content of impurity elements (the combined concentration of Fe, Al, Mg, Mn, Si, and B is $5.3 \times 10^{-2}$ %) makes it possible to obtain high-purity ingots, since the nonporous outer surface of the products made with them impedes the diffusion of impurities into the materials and increases the service life of the products at high temperatures (Fig. 1) [1 – 3].

In the production of material UPA-3, first Olilon-grade fibers (oxidized PAN fibers) are mechanically knit on dual-needle-bed knitting machine HDR-8 made by the "Karl Mayer" company (in Germany) to create cloth with a weave having a reticular structure — a tricot chainette with an oval mesh. Templates are then used to cut the cloth into the required elements, which are subsequently sewn to form the base of the future product. The base is affixed to a graphite pattern and placed in an electric vacuum furnace (EVF), where the base is saturated with PC to form the product's framework. The framework is stable but has minimal structural strength, which allows it to subsequently be compacted with PG.

Carbon fabrics based on viscose (type Ural-TM/4 [4] or TGN-2M [5]) are usually used as the reinforcing elements to make material UPA-4. They too are cut into the necessary elements with the use of templates and then sewn into packets of a prescribed thickness with Ural-NSh-24 threads [4]. After the packet is compressed and made secure by pressing it between perforated graphite slabs, by analogy with UPA-3 it is

---

[1] Scientific Research Institute of Graphite, Moscow, Russia.

subjected to pyrolysis with the use of mains gas in an EVF to obtain carbon-carbon panels which have the required dimensions, density, porosity, and thermophysical and mechanical properties.

When it is necessary to make products (parts) in the form of solids of revolution (for example) from fabrics or knitting, the elements of the future product are cut out with the use of templates and sewn onto a graphite pattern. These operations are repeated until a product of the necessary thickness has been formed. The entire packet of fabric (or knit) layers is then sewn together with carbon threads while it is still on the pattern. The sewn packet is placed in the EVF for deposition of the PC and PG, resulting in the formation of a shell that has a knit middle layer consolidated with PC and inner and outer layers comprised of PG. The physico-mechanical and thermophysical properties of the inner and outer layers are characterized by appreciable anisotropy.

It is known that internal stresses develop in such products after their compaction with PC and PG. These stresses are created due to the anisotropy that develops in the properties of the PG-coating as it cools from the final temperature during the deposition process (1800 – 2000°C) to room temperature.

## EXPERIMENTAL PART

To obtain statistical data for all of the specimens that were examined, we determined apparent density $\rho_a$, pycnometric density $\rho_p$, and open porosity $P_{open}$ by hydrostatic weighing in accordance with the method specified by the standard GOST 2409. During preliminary metrological certification of the method for graphites and other carbon materials, it was determined that the absolute errors in the determination of $\rho_a$ and $\rho_p$ are ±0.007 and ±0.002 g/cm$^3$ and that the absolute error of $P_{open}$ is ±0.3% [6].

Measurements were performed for a large number (200) of specimens with the use of standard isooctane (2,2,4-trimethylpentane, $C_8H_{18}$; GOST 12433) as the substituent. This compound has a low surface tension, $\sigma = 18.77 \times 10^{-3}$ N/m, at 20°C, and the temperature dependence of its density is known to within ±0.00005 g/cm$^3$ [7]. The specimens were saturated with the compound in a vacuum. Weighing was done with the 2004MP6 electronic microbalance made by the "Sartorius" company (Germany). The microbalance makes it possible to weigh 10-g and 100-g masses with an error of ±0.09 and ±0.2 mg, respectively.

As regards its effect on the human body, isooctane is considered to be a class-4 hazardous substance under the standard GOST 12.1.007 — in contrast to methyl alcohol and ethyl alcohol. The maximum allowable concentration of isooctane in the air of a work room is 300 mg/m$^3$.

The pore structure of the specimens of UPA-3 and UPA-4 was studied by the method of mercury pyrometry (MPM) [8 – 10]. Here, we determined the specific volume of the pores $V$ and the character of its distribution based on



**Fig. 1.** Products made of material UPA-3.

equivalent radii $R_{eqv}$ [8]: the volumes of the pore-traps (the bottle-shaped pores) $V^*$ and the volume of the pore-capillaries or transport pores $\Delta V = V - V^*$ [9 – 11], as well as the size of the largest pores in the material $R_{max}$ and the specific surface $S_{sp}$ (cylindrical-pore model). The volume of the pore-traps was determined either from the mass or volume of mercury remaining in the specimen after pressure was reduced from the final working pressure to atmospheric pressure or from the result obtained by weighing the specimen after it was removed from the dilatometer. The pore-traps and the other pores are connected to one another and to the outside surface of the specimen by the pore-capillaries.

The automated porosimeter "Auto Pore 9200" made by the company "Micromeritics" (U.S.) was used to store and analyze the information. The instrument was equipped with a microcomputer and the appropriate software. The capacitance method that the unit employs to determine the volume of mercury which penetrated the pores in the specimen under the influence of rising pressure has a resolution equal to ±1% of the capillary volumes in the dilatometer (which in the foreign literature is referred to as a penetrometer): 0.38, 1.1, and 1.8 cm$^3$. The resolution of the method with respect to pressure (the calculation of $R_{eqv}$ [8]) is ±10% of the scale of the vacuum gage (100 – 400 μm Hg) and ±1% of the complete scale of the low-pressure manometer (0 – 0.21 MPa) and high-pressure manometer (0 – 2.07, 2.07 – 27.6, 27.6 – 414 MPa) of the porosimeter.

Specimens of UPA-3 and UPA-4 with a cross section of $10 \times 10$ mm and a length in the range 20 – 30 mm were cut out from the manufacturing allowance (MA) of full-size products or from test tiles subjected to different amounts of pre-compression $Z = 16 - 10$ mm and compacted with PC (PG) for different periods of time $\tau = 360 - 990$ h.

The coefficient of gas permeability $K_g$ at 20°C, which characterizes the through (active) porosity of materials, was

determined by the "vacuum flow" method [12]: the metrologically certified method and unit in [13] were used to measure the rate of pressure increase in a pre-evacuated vessel that had a known capacity and was isolated from the atmosphere by a specimen of the test material having certain dimensions (diameter 36 mm and height 4 – 16 mm). The error of the determination for materials with $K_g \geq (12 \pm 4)$

$\times 10^{-5}$ cm²/sec: ±0.08 cm²/sec for $K_g \approx 0.13$; ±0.1 cm²/sec for $K_g \approx 1.8$; ±2 cm²/sec for $K_g \leq 13.3$. Intermediate values of $K_g$ were determined by interpolation. The relative error of $K_g \leq 12\%$.

The mechanical properties of the materials — ultimate strength in tension $\sigma_{tsn}$, compression $\sigma_{cr}$, bending $\sigma_{bnd}$, transverse shear $\sigma_{tsh}$, and longitudinal shear $\sigma_{lsh}$ — were evalu-

**TABLE 1.** Characteristics of the Pore Structure of Tile Specimens of Material UPA-4 Subjected to Different Degrees of Compression and Compacted with Pyrolytic Carbon for Different Periods of Time

| Specimen | $\tau$, h, PC | Density, g/cm³ | | Open porosity, % | Pore volume, cm³/g | | | $R_{max}$, μm | $S_{sp}$, m²/g |
|---|---|---|---|---|---|---|---|---|---|
| | | $\rho_a$ | $\rho_c$ | | $V$ | $V^*$ | $\Delta V$ | | |
| *Degree of pre-compression Z = 16 mm for the series-2 tiles* | | | | | | | | | |
| 1 | 360 | 1.19 | 1.591 | 25.20 | 0.253 | 0.055 | 0.198 | 55.10 | 11.05 |
| 2 | 450 | 1.16 | 1.586 | 26.86 | — | — | — | — | — |
| 3 | 540 | 1.16 | 1.580 | 26.58 | — | — | — | — | — |
| 4 | 630 | 1.17 | 1.582 | 26.04 | — | — | — | — | — |
| 6 | 720 | 1.19 | 1.585 | 24.92 | 0.246 | 0.116 | 0.130 | 54.89 | 7.40 |
| 7 | 810 | 1.21 | 1.577 | 23.27 | — | — | — | — | — |
| 7 | 810 | 1.21 | 1.576 | 23.22 | — | — | — | — | — |
| 8 | 900 | 1.23 | 1.601 | 23.17 | — | — | — | — | — |
| 9 | 990 | 1.24 | 1.598 | 22.40 | 0.229 | 0.065 | 0.164 | 55.51 | 9.01 |
| Mean $\bar{x}$ | | 1.20 ± 0.03 | 1.586 ± 0.009 | 24.63 ± 1.66 | 0.243 ± 0.012 | 0.079 ± 0.033 | 0.164 ± 0.034 | 55.17 ± 0.32 | 9.15 ± 1.83 |
| Coefficient of variation $w$, % | | 2.5 | 0.8 | 6.7 | 4.9 | 41.8 | 20.7 | 0.6 | 20.0 |
| *Degree of pre-compression Z = 13 mm for the series-3 tiles* | | | | | | | | | |
| 1 | 360 | 1.17 | 1.543 | 24.17 | 0.255 | 0.069 | 0.186 | 55.51 | 7.70 |
| 2 | 450 | 1.20 | 1.540 | 22.08 | — | — | — | — | — |
| 4 | 540 | 1.24 | 1.550 | 20.00 | — | — | — | — | — |
| 5 | 630 | 1.25 | 1.556 | 19.67 | — | — | — | — | — |
| 6 | 720 | 1.27 | 1.570 | 19.11 | 0.187 | 0.053 | 0.134 | 54.89 | 12.00 |
| 7 | 810 | 1.29 | 1.576 | 18.15 | — | — | — | — | — |
| 8 | 900 | 1.32 | 1.596 | 17.29 | 0.141 | 0.104 | 0.037 | 55.10 | 10.30 |
| 9 | 990 | 1.36 | 1.596 | 14.79 | — | — | — | — | — |
| Mean $\bar{x}$ | | 1.26 ± 0.06 | 1.566 ± 0.022 | 19.41 ± 2.87 | 0.194 ± 0.057 | 0.075 ± 0.057 | 0.119 ± 0.076 | 55.17 ± 0.32 | 10.00 ± 2.17 |
| Coefficient of variation $w$, % | | 4.9 | 1.4 | 14.8 | 29.4 | 76.0 | 63.9 | 0.6 | 21.7 |
| *Degree of pre-compression Z = 10 mm for the series-5 tiles* | | | | | | | | | |
| 1 | 360 | 1.20 | 1.536 | 21.88 | 0.230 | 0.069 | 0.161 | 54.89 | 9.57 |
| 2 | 450 | 1.24 | 1.531 | 19.01 | — | — | — | — | — |
| 4 | 540 | 1.28 | 1.540 | 16.88 | — | — | — | — | — |
| 6 | 720 | 1.28 | 1.535 | 16.61 | 0.166 | 0.051 | 0.115 | 54.89 | 11.70 |
| 7 | 810 | 1.32 | 1.531 | 13.78 | — | — | — | — | — |
| 9 | 990 | 1.37 | 1.542 | 11.15 | 0.111 | 0.043 | 0.068 | 36.87 | 12.25 |
| Mean $\bar{x}$ | | 1.28 ± 0.06 | 1.536 ± 0.005 | 16.55 ± 3.78 | 0.169 ± 0.060 | 0.054 ± 0.013 | 0.115 ± 0.047 | 48.88 ± 10.40 | 11.17 ± 1.42 |
| Coefficient of variation $w$, % | | 4.6 | 0.3 | 22.8 | 35.5 | 24.1 | 40.9 | 21.3 | 12.7 |

ated on specimens with dimensions of $10 \times 10 \times 20$ mm and $8 \times 8 \times 40$ mm. The properties were determined on universal testing machines "Zwick-1474" made by the "Zwick/Roell" company (Germany) and "Instron" (made in Great Britain). The relative error of the test results was $\pm 1\%$.

## RESULTS AND DISCUSSION

Table 1 shows the density, porosity, and pore-structure parameters of specimens of material UPA-4 in relation to the values of $Z$ and $\tau$. The specimens were cut from the MA of products or from tiles. The principal axis of symmetry of the specimens (along the specimens) was parallel to the $y$ axis (the warp of the fabric), the $x$ axis (the weft of the fabric), or the $z$ axis — perpendicular to the layers of fabric, i.e. perpendicular to the thickness of the tile.

It follows from Table 1 that due to the high degree of stability of the values of $\rho_p$ (the coefficient of variation $w$ was equal to 0.8, 1.4, and 0.3% for tiles with $Z = 16$, 13, and 10 mm, respectively), there is a direct relation between $\rho_a$ and $P_{open}$ for a sample size $n = 22$ specimens. This relation is expressed by the equation $P_{open} = -65.29\rho_a + 101.68$, with the correlation coefficient $r = -0.97$. The same type of relationship also exists between $V$ and $\rho_a$ for the specimens studied by MPM ($n = 9$) and is described by the equation $V = -0.767\rho_a + 1.159$, with $r = -0.98$.

As regards the volume of transport pores $\Delta V$ — which serve as pathways for the delivery of mains gas into the volume of the pore structure of the tiles to deposit PC — it decreases with an increase in $Z$ and $\tau$. This significantly reduces the effectiveness of the compaction process, as is illustrated by the slow decrease in the porosity of the tile specimens of series 2: $P_{open}$ decreased by ~2.8% and $V$ decreased by 0.034 cm³/g. It can be seen from Fig. 2 that increases in $Z$ and $\tau$ were accompanied by decreases in $P_{open}$ by roughly 9.4% and in $V$ by 0.114 cm³/g for the tile specimens of series 3, while $P_{open}$ decreased 10.7% and $V$ declined 0.119 cm³/g for the tile specimens of series 5. There were also reductions in the value of $\rho_p$ (from 1.586 to 1.566 and 1.536 g/cm³, respectively) due to coverage of the mouth of the pore-traps by layers of PC deposited on their surface. This development converts the pore-traps into closed pores [14] that are inaccessible to methane, isooctane, and mercury (in the case we are examining).
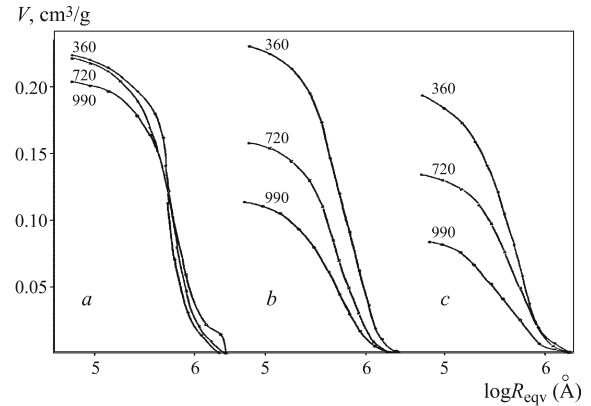


**Fig. 2.** Character of the distribution of $V$ in a Poiseuille-pore region with $R_{eqv} \geq 3.5$ µm for tile specimens of material UPA-4 subjected to different degrees of compression $Z$ ($a$ — 16; $b$ — 13; $c$ — 10 mm) and compacted for different periods of time $\tau$ (the times (h) are shown next to the curves); $a, b, c$) tile specimens of series 2, 3, and 5, respectively.
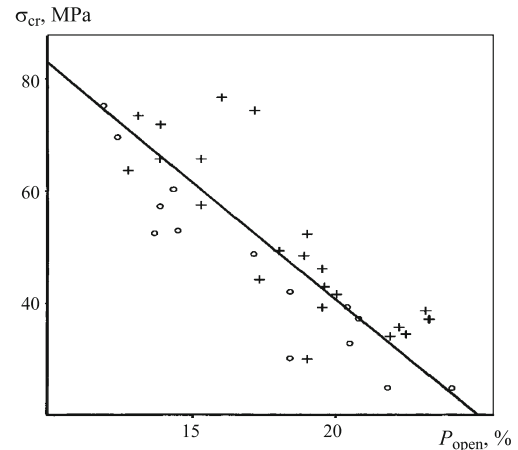


**Fig. 3.** Dependence of $\sigma_{cr}$ on $P_{open}$ for UPA-4 specimens cut out along the axial (+) and circumferential (O) directions.

Figure 2 shows structural curves of the distribution of $V$ with respect to the dimensions of $R_{eqv}$. The data in the figure covers only the region occupied by coarse pores (Poiseuille pores, in accordance with the classification in [15, 16]) with $R_{eqv} \geq 3.5$ µm in specimens of UPA-4 cut out from three batches of tiles that underwent different degrees of compression $Z$ and were compacted with PC for 360, 720, and 990 h,

**TABLE 2.** Arithmetic Mean Values of the Density, Porosity, and Ultimate Compressive Strength of Specimens of Material UPA-4

| Direction in which the specimens were cut out | Density, g/cm³ | | Open porosity $P_{open} \pm s$, % ($w$, %) | Ultimate compressive strength $\overline{\sigma}_{cr} \pm s$, MPa ($w$, %) | Number of specimens $n$ |
|---|---|---|---|---|---|
| | $\overline{\rho}_a \pm s$ ($w$, %) | $\overline{\rho}_p \pm s$ ($w$, %) | | | |
| Along the $y$ axis (axial) | 1.28 ± 0.05 (4.2) | 1.564 ± 0.011 (0.7) | 18.12 ± 3.25 (18) | 50.07 ± 14.87 (29.7) | 22 |
| Along the $x$ axis (circumferential) | 1.29 ± 0.07 (5.2) | 1.556 ± 0.014 (0.9) | 17.31 ± 4.00 (23) | 45.16 ± 15.66 (34.7) | 14 |

**TABLE 3.** Strength Indices of Material UPA-4 Based on Knitting and Fabric

| Indices | Ultimate strength, MPa | | | | |
|---|---|---|---|---|---|
| | $\sigma_{cr}$ | $\sigma_{tsn}$ | $\sigma_{bnd}$ | $\sigma_{tsh}$ | $\sigma_{lsh}$ |
| *Material UPA-4 based on knitting* | | | | | |
| Direction in which specimens were cut out: | | | | | |
| axial, *y*: | 62.6 ± 14.1 | 18.9 ± 3.4 | 52.7 ± 19.9 | 6.3 ± 1.4 | 8.8 ± 2.9 |
| *n* | 77 | 12 | 53 | 28 | 21 |
| *w*, % | 2.5 | 18.0 | 37.8 | 22.2 | 33.0 |
| circumferential, *x*: | 55.6 ± 11.1 | 17.8 ± 4.4 | 40.4 ± 10.8 | 5.4 ± 1.4 | 8.3 ± 1.5 |
| n | 84 | 7 | 37 | 19 | 15 |
| *w*, % | 20.0 | 24.7 | 26.7 | 25.9 | 18.1 |
| Anisotropy | 1.13 | 1.06 | 1.30 | 1.18 | 1.06 |
| *Material UPA-4 based on fabric* | | | | | |
| Direction in which specimens were cut out: | | | | | |
| axial, *y*: | 80.7 ± 77.7 | 57.2 ± 24.0 | 51.6 ± 35.3 | — | — |
| *n* | 137 | 68 | 193 | — | — |
| *w*, % | 96.3 | 42.0 | 68.4 | — | — |
| circumferential, *x*: | 56.1 ± 30.3 | 58.2 ± 55.2 | 38.5 ± 16.4 | — | — |
| *n* | 142 | 52 | 115 | — | — |
| *w*, % | 54.0 | 94.9 | 42.6 | — | — |
| Anisotropy | 1.44 | 0.98 | 1.34 | — | — |
| Ratio of the elastic moduli along the *y* and *x* axes $E^y/E^x$, GPa | 19.9/14.9 | 19.3/12.2 | 21.5/18.1 | — | — |
| Anisotropy | 1.34 | 1.58 | 1.19 | — | — |

respectively (see Table 1). Such pores accounted for >90% of $V$ in the tile specimens of series 2, from 74 to 84% in the specimens of series 3, and from 80 to 90% in the specimens of series 5.

It follows from the character of the curves that describe the distribution of $V$ with respect to $R_{eqv}$ (see Fig. 2*a*) that the rate of the process of consolidation of the tiles ($P_{open}$ equal to roughly 25%) was very low; there was almost no increase in density, $P_{open}$ decreased by 0.3%, and it took a very long compaction time (630 h) to achieve a 0.3% reduction in $P_{open}$ and a 0.07 cm³/g decrease in $V$. Such a process cannot be considered profitable.

A decrease in the thickness of the tiles by just 3 mm sharply altered the character of the compaction operation. For example, an additional 360 h of compaction with PC (specimens 1 – 6 of tile series 3) was accompanied by a decrease in $V$ by roughly 0.07 cm³/g and a 5% reduction in $P_{open}$. Here, $\Delta\rho_a$ increased by 0.1 g/cm³. The operation proceeded at a higher rate for the denser material (the tiles of series 5) than for the series-3 tiles, as can be seen from the character of the curves that show the distribution of $V$ with respect to $R_{eqv}$ (Fig. 2*c*).

In addition, an analysis of specimens of another batch (4 tiles) with different values of $Z$ and $\tau$ showed that the specimens with the highest density and least porosity were those whose axis was parallel to the direction of the *y* axis (the ax-

ial direction; the number of specimens $n = 39$): $\bar{\rho}_a = 1.39 \pm 0.03$ g/cm³; $P_{open} = 3.7 \pm 0.9\%$. Here, the relationship between $P_{open}$ and $\rho_a$ is expressed by the equation

$$P_{open} = -24.7\rho_a + 38.01, \, r = 0.88.$$

The indices were worse for the specimens cut out parallel to the *x* axis (circumferential direction, $n = 42$): $\bar{\rho}_a = 1.36 \pm 0.03$ g/cm³, $P_{open} = 4.3 \pm 0.9\%$, while the relationship $P_{open} f(\rho_a)$ was weaker:

$$P_{open} = -28.01\rho_a + 42.46, \, r = 0.78.$$

An analysis of the next batch of material UPA-4 (5 tiles) showed that the specimens ($n$ equal to 22 specimens) whose axis was parallel to the *z* axis had $\bar{\rho}_a = 1.32 \pm 0.02$ g/cm³ and $P_{open} = 14.1 \pm 1.3\%$, while the specimens whose axis was parallel to the *y* axis had values of $1.23 \pm 0.03$ and $18.2 \pm 1.9$, respectively. The relationship between $P_{open}$ and $\rho_a$ for these groups of specimens is expressed by the equations:

$$P_{open} = -64.94\rho_a + 99.77, \, r = -0.95,$$
$$P_{open} = -56.88\rho_a + 89.07, \, r = -0.94.$$

**TABLE 4.** Density, Open Porosity, and Gas Permeability of Material UPA-4*

| Specimen | Sector in which specimen was cut out | Density, g/cm³ $\rho_a$ | $\rho_p$ | Open porosity $P_{open}$, % | Coefficient of gas permeability $K_g$, cm²/sec |
|---|---|---|---|---|---|
| 6 | 3 | 1.28 | 1.566 | 18.26 | 20.79 |
| 10 | 3 | 1.26 | 1.570 | 19.75 | 21.01 |
| 38 | 3 | 1.22 | 1.566 | 22.10 | 22.23 |
| 10 | 4 | 1.26 | 1.566 | 19.54 | 20.59 |
| 11 | 4 | 1.24 | 1.567 | 20.87 | 20.33 |
| 12 | 4 | 1.24 | 1.567 | 20.88 | 19.91 |
| 1 | 20 | 1.23 | 1.585 | 22.40 | 17.76 |
| 2 | 20 | 1.23 | 1.579 | 22.10 | p12.00 |
| 3 | 20 | 1.23 | 1.583 | 22.30 | 21.65 |
| 4 | 20 | 1.23 | 1.577 | 22.00 | p14.84 |
| 5 | 20 | 1.24 | 1.583 | 21.67 | 9.58 |
| 40 | 22 | 1.27 | 1.580 | 19.62 | 15.26 |
| 47 | 22 | 1.23 | 1.578 | 22.05 | 18.30 |
| 50 | 24 | 1.27 | 1.603 | 20.77 | 14.31 |
| 52 | 24 | 1.27 | 1.606 | 20.92 | 13.72 |
| Average | | 1.25 | 1.578 | 21.02 | 18.11 |
| s | | ±0.02 | ±0.013 | ±1.25 | ±3.81 |
| w, % | | 1.6 | 0.8 | 5.9 | 21.0 |

* $\rho_a$, $\rho_p$, and $P_{open}$ were determined for 15 specimens and $K_g$ was determined for 13 specimens.
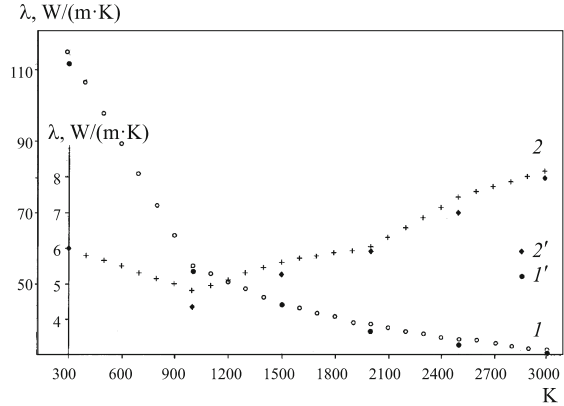


**Fig. 4.** Temperature dependence of thermal conductivity λ measured along the axial direction (*1*) and in the direction perpendicular to the thickness (fabric layers, *2*) of material UPA-4; the temperature dependence of thermal conductivity was also measured parallel (*1′*) and perpendicular (*2′*) to the surface of material UPA-3 on which PG was deposited.

It must be emphasized that we are discussing "hidden" porosity, which is discovered when specimens made from the MA of products (tiles) are cut open to determine their properties. The outside surface of the specimens was almost free of pores, as noted above.

Table 2 shows values of $\overline{\rho}_a$, $\overline{\rho}_p$, $P_{open}$, ultimate compressive strength $\overline{\sigma}_{cr}$, and the rms errors $s$ and $w$ [17] for

specimens cut from four batches of tiles (6, 8, 9, and 12) of material UPA-4.

The anisotropy of strength was equal to 1.11, and the dependence of $\sigma_{cr}$ on $P_{open}$ for the specimens cut out parallel to the $x$ axis is expressed by the equation $\sigma_{cr} = -3.87P_{open} + 108.69$, with $r = -0.94$; the dependence was less pronounced for the specimens cut out parallel to the $y$ axis ($n = 22$): $\sigma_{cr} = -3.64 P_{open} + 120.26$, $r = -0.85$. However, the indices of the properties of these specimens were more stable. This is shown in Fig. 3, from which it follows that the value of $\sigma_{cr}$ for the specimens whose axis was parallel to the $y$ axis was ~10% greater than for the specimens having their axis parallel to the $x$ axis: all of the points in the circumferential direction lie on or below the straight line.

Other strength indices of material UPA-4, based on knitting and fabric (Ural-T-22), were determined on specimens of standard shape and dimensions by using government stan-

**TABLE 5.** Density, Porosity, and Gas Permeability of Elements of Parts Made of Materials UPA-4 and UPA-3

| Object studied | Number of specimens $n$ | Density ± s, g/cm³ $\overline{\rho}_a$ | $\overline{\rho}_p$ | Porosity $P_{open}$ ± s, % | Coefficient of gas permeability $K_g$ ± s, cm²/sec |
|---|---|---|---|---|---|
| | | *Material UPA-3* | | | |
| Fragment | | | | | |
| 3 | 6 | 1.35 ± 0.01 | 1.546 ± 0.001 | 12.70 ± 0.46 | 2.34 ± 0.45 |
| w, % | | 0.5 | 0.1 | 3.7 | 19.1 |
| 16 | 13 | 1.31 ± 0.02 | 1.575 ± 0.007 | 17.05 ± 1.43 | 10.29 ± 3.51 |
| w, % | | 1.5 | 0.4 | 8.4 | 34.2 |
| | | *Material UPA-4* | | | |
| Part | 10 | 2.03 ± 0.02 | 2.082 ± 0.025 | 2.91 ± 0.53 | (2.93 ± 0.90) × 10–3 |
| w, % | | 1.3 | 1.2 | 18.2 | 30.9 |

**TABLE 6.** Average Values of the CLE ($\alpha$) of Material UPA-3 in Relation to Measurement Temperature

| Direction of measurement | CLE, $10^{-6}$ $K^{-1}$, measured at different temperatures, °C | | | | | | |
|---|---|---|---|---|---|---|---|
| | 20 – 200 | 20 – 400 | 20 – 600 | 20 – 800 | 20 – 1000 | 20 – 1500 | 20 – 2000 |
| Parallel to the deposition surface ($\alpha^{\parallel}$) | 0.5 – 0.7 | 1.1 – 1.2 | 1.2 – 1.6 | 1.3 – 1.8 | 1.3 – 2.1 | 1.7 – 2.4 | 2.0 – 3.0 |
| Perpendicular to the deposition surface ($\alpha^{\perp}$) | 8.8 – 9.0 | 8.8 – 9.7 | 8.9 – 9.7 | 9.0 – 9.8 | 9.6 – 9.8 | 10.5 | 11.8 |

dards or methods developed at the institute. The results are shown in Table 3. A material based on knitting is less isotropic and has more stable (based on $w$) strength properties than specimens with a fabric filler, which have a high ultimate tensile strength for specimens cut out in either direction and similar values of $\sigma_{bnd}$ and $\sigma_{cr}$ in the circumferential direction. The ultimate compressive and tensile strengths of specimens of the fabric-based material that were cut parallel to the $y$ axis were greater than the corresponding values for the knit specimens by factors of 1.3 and 3, respectively.

The value of $K_g$ was measured on 36-mm-diam. specimens of UPA-4 with a thickness corresponding to 5 sectors of the MA for the given part. The values of $\rho_a$, $\rho_p$, and $P_{open}$ were determined beforehand. The results are shown in Table 4.

It follows from the data in Table 4 that the part made of material UPA-4 was distinguished by high porosity ($\overline{\rho}_a < 1.4$ g/cm$^3$) and the existence of holes at the locations where the packet of fabric layers was penetrated by the "Ural-NSh-24" thread that was used to sew it. These holes, which were not completely filled with PC, were the reason for the high permeability of the material. Their presence made it impossible to find a correlation between $K_g$ and/or $P_{open}$ and $\rho_a$, since the existence of even one such hole on the surface of the specimens sharply increases the material's value of $K_g$.

A similar pattern was seen when we analyzed the results of measurements of $K_g$ for two batches of 36-mm-diam., 3.0 – 3.5-mm-thick specimens from fragment 3 ($n = 6$) and fragment 16 ($n = 13$) of parts made of material UPA-4. Table 5 shows the results and data for parts based on material UPA-3 ($n = 10$).

For the specimens from fragment 3 of UPA-4, the dependence of $P_{open}$ on $\rho_a$ has the form $P_{open} = -73.59\rho_a + 112.05$, $r = -1.0$. Unfortunately, no relationship was found between $K_g$, $P_{open}$, and $\rho_a$. For the specimens from fragment 16, the relation between $P_{open}$ and $\rho_a$ is expressed by the equation $P_{open} = -74.5\rho_a + 114.5$, $r = -0.96$. The connection between $K_g$ and $P_{open}$ is very weak ($r = -0.64$), for the reasons mentioned above ($\overline{\rho}_a < 1.4$ g/cm$^3$; the presence of holes on the specimen surface that were partially filled with PC).

When it was necessary to increase the thickness of products made of UPA-3, in certain cases several parts were joined together into a single product with the use of special adhesives [18]. The hermeticity of these products was evaluated based on the quantity $K_g$. For example, $K_g =$ $(3.36 \pm 0.53) \times 10^{-2}$ cm$^2$/sec for a sample comprised of disk-shaped specimens ($n = 4$) that had a diameter of 36 mm and height of 10 mm and whose axis of symmetry was parallel to the joined layers (and the fluid flow). For a sample of specimens whose axis was perpendicular to their thickness, $\overline{K}_g$ changed within the range from $(2.68 \pm 1.44) \times 10^{-3}$ ($n = 6$) to $(4.07 \pm 0.62) \times 10^{-4}$ cm$^2$/sec ($n = 4$), i.e. the gas permeability of the working surface was 1 – 2 orders of magnitude lower than for the adhesively joined surfaces.

Figure 4 shows data on the thermal conductivities of specimens of material UPA-4 cut out in different directions. As reference data, Table 6 presents values of the coefficient of linear expansion (CLE) for material UPA-3.

Thus, the anisotropy $\overline{\alpha}$ $\alpha^{\perp}/\alpha^{\parallel}$ for each of the 7 ranges of measurement of $\alpha$ ($n = 14$) was $7.4 \pm 3.7$ ($w = 49.5\%$). This result is much more typical of pure PG: $\alpha_c/\alpha_a > 1000, > 210$, and 13 – 18 for the temperature ranges 293 – 400, 293 – 800, and 293 – 2300 K [19, 20], respectively. In our case, the anisotropy $\alpha$ was smoothed by the fact that there was a knit carbon-fiber-based reinforcing filler between two layers of PG.

## CONCLUSION

An analysis was made of the changes that occur in the density, pore structure, and mechanical strength of materials UPA-4 and UPA-3 in relation to the degree of preliminary compression of the tiles (frameworks) and the length of time they are compacted with pyrolytic carbon and/or graphite.

It was shown that it is inadvisable to use weakly pre-compressed tiles based on carbon-fiber fabrics with different textile structures to make carbon-carbon composites due to the high initial open porosity (>25%) and the fact that the material contains through pores whose ends are not closed by the PC matrix when the packets are pierced. These factors increase the gas permeability of the finished product.

The high degree of stability of the values of $\rho_p$ of the material ensure a close correlation between $P_{open}$ and $\rho_a$, with $r \geq -0.94$. A somewhat weaker correlation exists between $\sigma_{cr}$ and $P_{open}$ ($r$ from $-0.84$ to $-0.94$), the closeness of this correlation being affected by the direction in which the specimens are cut out for testing.

Knitting-based material UPA-4 exhibits less anisotropy with respect to several strength characteristics than does the fabric-based variant. It is distinguished by high tensile strength in specimens cut out in the axial and circumferential

directions and high compressive strength in the circumferential direction. The two materials have similar values for ultimate strength in bending.

Material UPA-3 is characterized by high density and low porosity. Its gas permeability is 3 – 5 orders of magnitude lower than that of material UPA-4.

## REFERENCES

1. *Reinforced Pyrolytic Carbon UPA-3E: Prospectus NIIgrafit*, Vneshtorgizdat, Moscow (19S89). Izd. No. 6676MB.
2. *Reinforced Pyrolytic Carbon of Grade UPA-3E. Production Data: information sheet*, NIIgrafit, Moscow.
3. *Properties of Structural Materials Based on Carbon: Handbook* [in Russian] (Ed: V. P. Sosedov). Metallurgiya, Moscow (1975).
4. M. E. Kazakov, "Production of fibrous carbon materials based on viscose fibers," in: *Chemical Reinforcing Fibers for Composite Materials* [in Russian] (Ed: G. I. Kudryavtsev). Khimiya, Moscow (1992), pp. 263 – 291.
5. *Graphitized Fabric TGN-2M: Prospectus of NIIgrafit*, Vneshtorgizdat, Moscow (1989). Izd. No. 6673MB.
6. G. M. Butyrin, A. I. Polozhikhin, L. A. Zimina, et al., "Use of isooctane in determining the open porosity of different carbon materials," in: *Carbon Materials: Symposium*, NIIgrafit, Moscow (1991), pp. 138 – 140.
7. N. B. Vargaftik, *Handbook of the Thermophysical Properties of Gases and Liquids* [in Russian], Nauka, Moscow (1972).
8. E. W. Washburn, "Note on a method of determining the distribution of pore size in a porous material," *Proc. N. A. S. Physics*, **7**, 115 – 116 (1921).
9. G. M. Butyrin, *High-Porosity Carbon Materials* [in Russian], Khimiya, Moscow (1976).
10. T. G. Plachenov and S. D. Kolosentsev, *Porometry* [in Russian], Khimiya, Leningrad (1988).
11. L. A. Zimina and G. M. Butryin, "Study of the pore structure of large electrodes by the method of mercury porometry," *Tsvetn. Met.*, No. 8, 54 – 57 (1978).
12. J. F. Hewitt, "Gas transport in graphite," in: *Chemical and Physical Properties of Carbon* [Russian translation] (Ed.: F. Walker), Mir, Moscow (1969), pp. 78 – 124.
13. G. M. Butyrin, *Method of Determining the Coefficient of Gas Permeability of Carbon Materials*, MI 4807-129–86. NIIgrafit, Moscow (1986).
14. L. M. Manocha, "High performance carbon-carbon composites," *Sadhana*, No. 28, 349 – 358 (2003).
15. G. M. Butyrin, M. I. Rogailin, and E. F. Chalykh, "Pore structure of artificial graphite and its classification based on specific volume and pore size," *Khim. Tverd. Tela*, No. 1, 131 – 146 (1971).
16. M. I. Rogailin, G. M. Butyrin, and E. F. Chalykh, "Classification of industrial graphite porous structure by specific volume and pore sizes," in: *Pore Structure and Properties of Materials: Proc. Intern. Symp.*, IUPAC. Prague, Sept. 18 – 21, 1973, Rep. Part II, Academia, Prague (1974), pp. A103 – A110.
17. A. N. Zaidel', *Elementary Estimates of Measurement Errors* [in Russian], 3rd Ed., Nauka, Leningrad (1968).
18. G. A. Kravetskii, L. T. Anikin, A. V. Demin, et al., "Adhesive bonding of carbon and ceramic materials," in: *Proc. 2nd Intern. Conf. on High-Temp. Ceramic-Matrix Composites*, Santa Barbara, Aug. 21 – 24, 1995, Amer. Ceram. Soc. pp. 465 – 470.
19. A. V. Emyashev and L. V. Lavrova, "Structural parameters and certain properties of pyrolytic graphite alloyed with boron or silicon," in: *Structural Materials Based on Graphite* [in Russian], Metallurgiya, Moscow (1967), Vol. 3, pp. 74 – 79.
20. B. K. Dymov, A. I. Lutkov, V. I. Volga, et al., "Thermal conductivity, resistivity, and thermal expansion of graphite-based structural materials in the temperature range 100 – 3000 K," *Ibid*, (1971), Vol. 6, pp. 45 – 58.